FACULTY OF INFORMATION TECHNOLOGY AND ELECTRICAL ENGINEERING

Aleksandra Zienkiewicz

BLOOD PRESSURE ESTIMATION USING PULSE TRANSIT TIME MODELS

Master's Thesis
Degree Programme in Computer Science and Engineering
November 2017

ABSTRACT

Blood pressure (BP) is an important indicator of human health. Common methods for measuring BP continuously are either invasive, intermittent or they require using a cumbersome cuff. Pulse Transmit Time (PTT) -based measurement can be an alternative for such methods, as it ensures continue and non-invasive monitoring. However, since the method is indirect, it requires careful modelling of PTT-BP relation. In this thesis, three approaches of BP estimation from PTT are tested: linear regression, nonlinear Moens and Korteweg model and nonlinear model developed by Gesche. In the experiments, cardiovascular pulses for PTT were sensed using two fiber optics based accelerometers developed at the University of Oulu.

To evaluate feasibility of presented models, the results were compared with reference BP values, measured using methods accepted for the commercial use. There were two groups of data. One was compared with BP measured using invasive catheter. Second group was compared with BP measured using volume clamp method. Obtained results suggest, that the presented calculation methods in present state still require further development in order to provide accurate BP values, however, they can be potentially used for observation of BP changes.

Keywords: blood pressure, non-invasive, pulse transit time, pulse wave velocity

TABLE OF CONTENTS

FOREWORD

I never dreamed that my primarily short, three-months trip to visit Finland will have such long-term and life changing effects. University of Oulu is a great environment for students and researchers; for me personally it is also a place where I could challenge myself, find new passions and friendships. I believe I have learned a lot and I am proud for having a chance to study and work in such a great community.

In this thesis, I present the first stage of my work on modeling of blood pressure from pulse transit time measured with fiber optics accelerometer sensors. I have introduced the importance of blood pressure measurements and currently available methods. I hope that I have also convincingly justified the relevance of continuous non-invasive blood pressure measurement techniques, and why they can be so useful for both medical doctors and researchers. Fiber optics accelerometer sensors have additional asset of full compatibility with brain imaging methods, which is why I strongly believe in the research potential of this technique. I decided to continue my work on this topic on the post-graduate studies. Biomedical engineering is a dynamically growing discipline, especially in Finland, and I am happy to be a part of this field.

I would like to express my deepest gratitude to both of my advisors. To Professor Tapio Seppänen who always had time to answer my questions, mobilized me to hard work when I needed it, and who has endless patience for his students. Also to Adjunct Professor Teemu Myllylä for his expertise, constructive feedback and, above all, for his friendship. Thank you for always believing in me.

My wonderful family always showed me the greatest support in my projects and ideas. Thank you for all the understanding, inspiration and love that you keep on giving me, no matter the distance between us.

University supervisor: Dr. Tech. Prof. Tapio Seppänen
Second examiner: D.Sc.(Tech.) Adj. Prof. Teemu Myllylä

Oulu, 27.11.2017

Aleksandra Zienkiewicz

ABBREVIATIONS

ACM	optomechanical accelerometer sensor
ACM1	ACM sensor placed on the chest
ACM2	ACM sensor placed on the neck
AP	arterial pressure
BP	blood pressure
BP_G	BP estimated using PTT and non-linear model presented by Gesche
BP_I	invasively measured SBP
BP_{LIN}	BP estimated using PTT and linear regression model
BP_{M-K}	BP estimated using PTT and Moens - Korteweg non-linear model
bpm	heartbeats per minute
CVD	cardiovascular disease
DBP	diastolic blood pressure
ECG	electrocardiogram
fMRI	functional magnetic resonance imaging
HR	heart rate
HR_{ACM1}	HR measured by ACM chest sensor
HR_{ACM2}	HR measured by ACM neck sensor
HR_{IBP}	HR measured by intra-arterial catheter
HR_{FIN}	HR measured by Finometer
HV	hyperventilation
IBP	invasive blood pressure measurement
MAP	mean arterial pressure
MEG	magnetoencephalography
MREG	magnetic resonance encephalography
MRI	magnetic resonance imaging
NIBP	non-invasive methods of blood pressure monitoring
P1 – P5	pulse components in Pulse Decomposition Analysis
PDA	Pulse Decomposition Analysis
PPG	photoplethysmogram
PTT	Pulse Transit Time
PWV	Pulse Wave Velocity
r	Pearson's correlation coefficient
SBP	systolic blood pressure
SD	standard deviation
SG	Savitzky-Golay filter
T13	time delay between the systolic and the iliac peak
d	distance between sensors
E	Young's modulus describing the elasticity of the arterial wall
E_0	zero pressure modulus
h	vessel wall thickness
P	pressure
r_0	inner radius of the vessel
α	vessel-dependent constant
ρ	blood density

1. INTRODUCTION

Blood pressure (BP) is an important indicator of heart and vessel condition. It is an essential element of every health monitoring system, since it may provide an important knowledge about patient's state and alarm about increased risk of developing a heart attack, stroke and other complications. For prevention and early diagnosis of hypertension and its associated complication, it is imperative to monitor and evaluate BP and its changes over time accurately and continuously [1].

Commonly available methods used in medical practice are based on catherization (continuous and reliable absolute BP value, but invasive solution) and sphygmomanometry (noninvasive, but cumbersome and provide intermittent readings), which means that they limit the quality of life of the patients and cannot be used 24 hours a day. There is a clear demand on user-friendly non-invasive BP monitoring device for various application areas. In particular, a continuous long-term BP monitoring method would give more comprehensive and reliable information about subject's health by enabling doctors to observe patients' BP changes in relation to physical and mental stress during a longer period of time. In addition, such device could be used in various clinical monitoring and medical research areas, for instance to study effects of medicines or cerebral autoregulation studies [2]. In brain research, understanding brain function in relation to BP more deeply is as well of great interest [3-7]. Moreover, blood flow-related dynamics in the brain are still relatively little examined, which is why they are now attracting the attention of developers of new measurement methods [8, 9].

In this thesis, the sensors for non-invasive continuous Pulse Transit Time (PTT) measurement were tested together with three mathematical models enabling estimation of BP from PTT. Setup with fiber optics based accelerometers used for measurements was developed at the University of Oulu [10]. It enables measurement of PTT, and thus indirect estimation of BP. PTT to BP conversion was done using three different models, obtained from the professional literature: linear model, Moens-Korteweg model and Gesche model. To evaluate the models, results were compared with the reference BP values, recorded simultaneously using approved devices. Results for all three models are shown in a study.

Structure of the thesis consists of following elements. Chapter 2 includes description of motivation for the study and background, where the basic information about cardiovascular system and BP are described . In Chapter 3, various techniques for measuring BP are presented, for instance catherization, and volume-clamp method. Basics of PTT utilization for BP estimation is introduced in this chapter as well. Description of measurement methods, signal processing methods and data analysis is presented in Chapter 4. These models are originally presented in literature [10-14] and here I evaluate feasibility of the models for continuous BP measurements. Chapter 5 contains results of the study, illustrated with exemplary plots. Observations and discussion are described in Chapter 6, and the conclusions on the study output is presented in Chapter 7. Final chapter includes also possible prospects of the tested method and suggested improvements.

2.   MOTIVATION AND BACKGROUND

Cardiovascular diseases (CVDs) are disorders of the heart and blood vessels. According to 2012 study conducted by World Health Organization, CVDs cause 31% of the deaths worldwide [15]. It is approximately 17.5 million people, which makes this group of disorders number one cause of death globally: more people die annually from CVDs than from any other cause. Therefore, researching and improving new methods of cardiovascular health assessment is of vital importance, as they can serve in CVDs prevention.

One of the key factors used in determining cardiovascular performance is blood pressure. In order to evaluate adequacy of various BP measurement methods, it is necessary to understand the underlying physiology of the human organism. Next sections contain basic information about cardiovascular system and blood pressure.

2.1.   The cardiovascular system

In order to enable better understanding of the topic, engineers often explain the structure of the cardiovascular system in terms of fluid mechanics. Following this approach, the working principle of the circulatory system can be described as a closed-loop hydraulic system [16]. It consists of the contracting heart serving as a pump, and vessels working as elastic pipelines that carry blood from the heart throughout the body. Simplified model of the human circulatory system is shown on Figure 1:
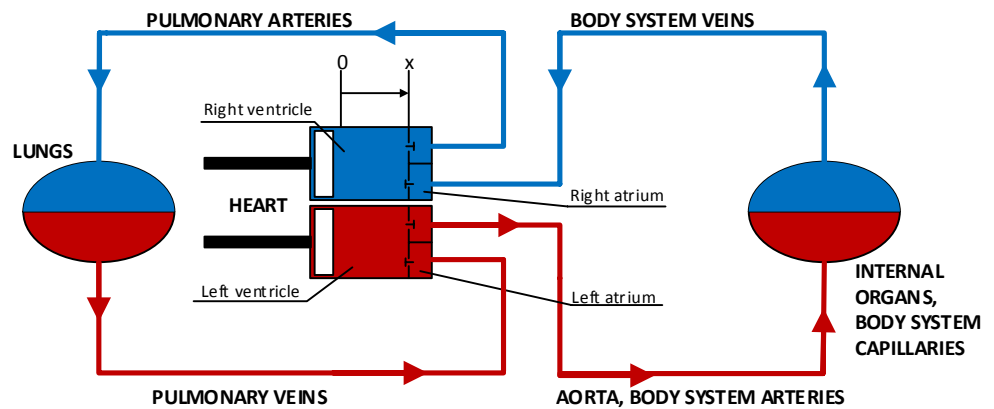

Figure 1. Simplified model of the human circulatory system [16].

Heart is divided into four chambers: the upper chambers are called atria, and the lower chambers are called ventricles. Blood low in oxygen return to the heart from the systemic circulation, enters the right atrium, then it is passed to the right ventricle. As next it is pumped into the pulmonary circulation, through the lungs where it receives oxygen and gives off carbon dioxide. Oxygenated blood returns to the left atrium and afterwards to left ventricle. From there it is ejected to the systemic circulation, where the oxygen is used and metabolized to carbon dioxide [17]. Four valves prevent backflow between the respective chambers and vessels.

Activity of the heart can be described with the amount of beats per minute (bpm), with the optimal heart rate (HR) of a healthy adult of approximately 60 to 90 bpm. Repeated, rhythmic contracting and relaxing guarantees blood motion through the vessels and create enough force to push blood through the major arteries, into the smaller arteries, and finally into the capillaries, where the porous walls allow the fluid exchange between blood and body tissue [18]. Circulating blood provides transportation and communication system between the body's cells and serves to maintain a relatively stable internal environment for optimum cellular activity [19].

2.2. Blood pressure

Term blood pressure refers to the force exerted by circulating blood on the walls of blood vessels [20]. It is usually used to indicate the arterial pressure (AP), due to the fact, that they are the vessels where the pressure is measured. BP values are reported in millimeters of mercury (mmHg).

2.2.1. Systolic and diastolic pressures

Due to the beating mechanism of the heart, AP is not a single value, but it varies between systolic and diastolic pressures. Systolic pressure (SBP) is the peak pressure, which occurs near the beginning of the cardiac cycle when the heart contracts and pushes the blood out. Diastolic pressure (DBP) is the minimum pressure in arteries, which occurs before the next contraction as the heart relaxes and blood fills in.

SBP and DBP levels vary from one heartbeat to another and throughout the day. They also change in response to stress, nutritional factors, drugs, disease and exercise [20]. Limits defining healthy level of BP are presented in Table 1, although it should be noted that values might slightly vary for different age range. If the pressure values exceed accepted limits, it is defined as hypertension (AP too high) or hypotension (AP too low).

Table 1 Classification of BP for adults [20].

Category	SBP [mmHg]	DBP [mmHg]
Hypotension	< 90	< 60
Normal	90-119	and 60 - 79
Prehypertension	120 - 139	or 80 - 89
Stage 1 hypertension	140 – 159	or 90 - 99
Stage 2 hypertension	≥ 160	or ≥ 100

Another commonly used parameter is mean arterial pressure (MAP). It can be calculated using SDB and DBP values, as shown in Formula (1):

$$MAP = \frac{SBP + 2 \cdot DBP}{3},$$
(1)

MAP is an estimation of average pressure forcing blood through the circulatory system. Its normal level varies from 96 to 100 mmHg.

2.2.2. Central and peripheral blood pressure

An important observation on BP is that its value varies significantly when measured in different sites of the arterial tree. It happens because the structure of the arterial walls differs between the central and the peripheral arteries. Central arteries (e.g. aorta) consist of more elastic fibers. Peripheral arteries (e.g. brachial, radial artery) are built of muscle cells and they tend to lose elasticity with aging. When the pressure wave travels from the heart down the arterial tree, it is reflected at any discontinuity of the arterial wall. As a result, the pressure waveform is the sum of a forward travelling waveform generated by left ventricular ejection and a backward travelling wave, the 'echo' of the incident wave, reflected at peripheral sites [21]. Because of the transmission of the pressure wave together with reflections, SBP can rise even for 10 – 14 mmHg when moving from the aorta to the brachial artery [21]. This effect is so-called 'pressure wave amplification'. The scope of the changes between the central BP and the peripheral BP depends partly on the stiffness of the arteries. Schematic representation of the BP level changes along the arterial tree is shown on Figure 2.
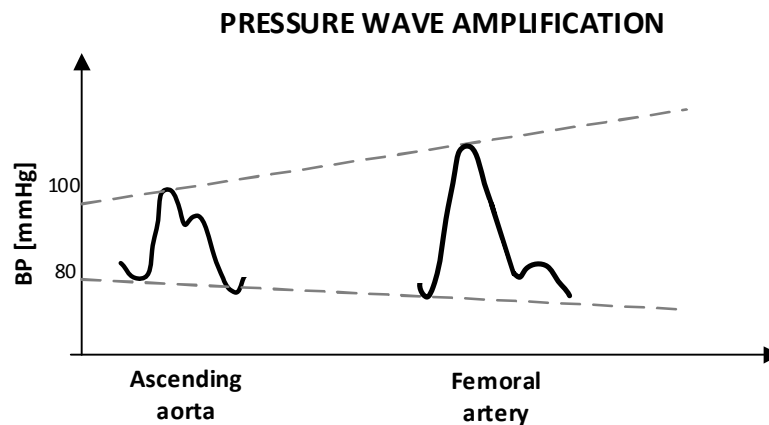

Figure 2. Example of BP level changes along arterial tree.

In clinical practice, the most commonly used methods for BP measurement are based on brachial artery occlusion, which can only measure peripheral BP (Section 3.2.1). However, the heart needs to pump against the aortic pressure, and thus central BP is more closely related to the pathophysiology of cardiovascular disease then peripheral BP. Because of pressure amplification effect, brachial BP cannot be considered as the perfect surrogate for central BP.

3. TECHNIQUES FOR MEASURING BLOOD PRESSURE

There are various techniques for measuring BP, but still the only non-invasive method considered as a 'gold standard' is auscultatory measurement with mercury sphygmomanometer [22]. Because of its numerous drawbacks, other methods are researched and tested. Classification of basic solutions in the field is presented on Figure 3 and their description is presented in Sections 3.1 and 3.2.
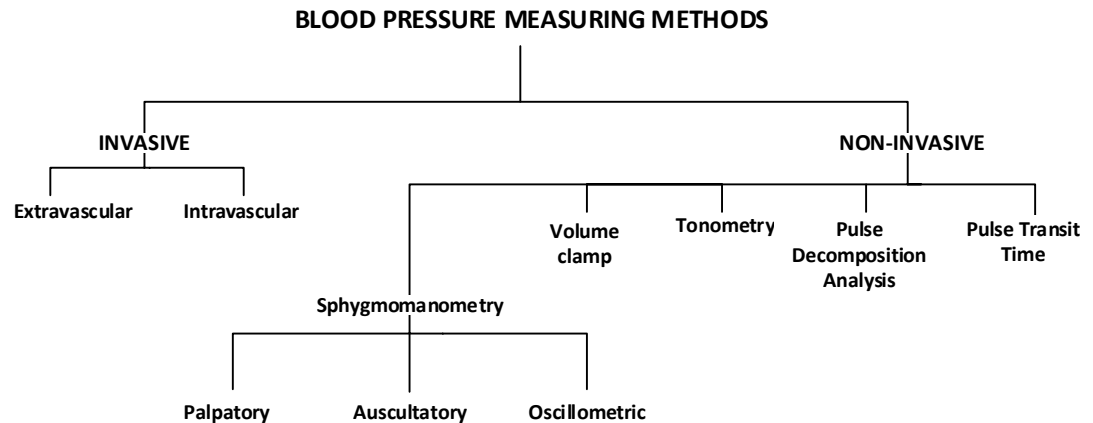

Figure 3. Classification of BP measuring methods.

3.1. Invasive BP measurement

Invasive methods of measuring BP involves insertion of a fluid-filled catheter (a flexible tube) and a pressure sensor inside of the artery. The most common sites are brachial and radial arteries but also other sites can be used e.g. femoral artery. Depending on the sensor placement, invasive systems can be divide into extravascular and intravascular.

1. Extravascular:

   The sensor is located behind the catheter and the vascular pressure is transmitted via this liquid-filled catheter.

2. Intra-vascular

   The sensor is located in the tip of the catheter. This way the hydraulic connection is replaced with an electrical or optical connection

   With the catheter BP can be measured continuously in real time and the method provides high quality result. However, this method has major drawbacks, which are significantly limiting its use. Insertion of the catheter is painful for the patient and requires auspices of the skilled medical staff, which additionally increases the procedural time and cost of the method. Invasive nature of the measurement implies high risk of hemorrhage, infection, blood clotting, embolism and a certain percent of mortality [19]. Furthermore, discomfort and anxiety of the patient due to the

placement of the catheter could raise the BP, giving readings that are not truly representative of the patient's condition [23]. Thus, invasive BP measurement (IBP) can only be justified in a limited number of cases. Non-invasive methods of BP monitoring (NIBP) were developed as an alternative, which allows to use safe BP monitoring in wide spectrum of applications, including routine screening procedures, research and home use.

3.2. Noninvasive techniques

NIBP measurement methods were developed as an alternative for IBP. The aim is to perform safe BP monitoring in wide spectrum of applications, including routine screening procedures, research and home use. However, non-invasive methods require indirect measurement of BP level, which challenges the researchers to design a method of high accuracy of the result.

3.2.1. Sphygmomanometry

Since XIX century, the most common methods of BP measurement are based on the occlusion of an artery. First sphygmomanometer ('sphygmo' – 'pulse' in Greek) with a brachial cuff, was introduced by Scipione Riva-Rocci. In his invention an inflatable elastic band (cuff) was wrapped around patient's arm and a glass manometer filled with mercury was connected to measure the cuff pressure.

Sphygmanometric measurement can be palpatory, auscultatory or oscillometric, depending on how they determine the pressure values. They are based on the same principle: to occlude an artery, measure the counterpressure and observe how it affects the characteristics of the blood flow in the artery [18].

Currently, because of toxic properties of mercury, the measurement of the pressure being actually applied to a brachial cuff is performed by either a mechanical transmission of the pressure to a circular scale (aneroid sphygmomanometer), or electronic pressure gauges (hybrid sphygmomanometer) [24]. However, mercury manometers still often serve as a golden standard in laboratories and hospitals.

PALPATORY METHOD
Riva – Roccis method allowed for easy and non-invasive measurement of systolic blood pressure. The measurement principles are following:

1. Cuff is placed on the patient's upper arm and filled with the air until the blood flow is entirely occluded.

2. During the slow deflation of the cuff, the artery is palpated until the pulse is felt again. In this moment, cuff pressure coincides with the systolic blood pressure.

Palpatory method can be inaccurate and requires experienced examiner.

AUSCULTATORY METHOD
Important limitation of palpatory method is that it could be used only for the SBP sensing. Thus, Riva-Roccis device was later combined with the findings of Nikolai

Korotkoff. Korotkoff observed, that by listening at the sounds generated by the arteries with a stethoscope one could determine specific blood flowing sounds occurring at different cuff pressures [24]. These two inventions established the basics of so-called auscultatory technique of BP measurement. The principle of this method is simple and is still applied in modern devices.

1. A stethoscope is placed over the artery below the cuff. No sound is audible when the blood flow is undistracted.
2. Cuff is filled with the air until the blood flow is entirely occluded. Cuff pressure is higher than the patient's systolic BP and there is no sound audible.
3. The brachial cuff is gradually deflated, until a first sound is heard at the stethoscope. Cuff pressure is then associated to the systolic pressure.
4. Deflating of the cuff continues, until any sound completely disappears from the stethoscope. Corresponding pressure is then associated to the diastolic pressure [24]. When the cuff pressure drops below diastolic pressure, the blood flow become undistracted again and no audible sound is produced.

Auscultatory method is highly dependent on the human examiner and his ability to detect and distinguish sounds.

OSCILLOMETRIC METHOD

Another occlusion measurement technique, which is fully automated, is oscillometric method. Instead of listening to the Korotkoff sounds, oscillometric devices are sensing tiny oscillations indicating the pulsatile blood volume in the artery [25]:

1. An electronic pressure sensor is fitted inside the cuff to detect magnitude of cuff pressure oscillations.
2. Cuff is filled with the air until the pressure exceeds systolic blood pressure. Cuff pressure vary periodically (oscillates) in synchrony with the cyclic expansion and contraction of the brachial artery.
3. The brachial cuff is gradually deflated. The cuff pressure, which cause an increased amplitude of oscillation are associated with SBP value.
4. Deflating of the cuff continues. Oscillation with the greatest amplitude has been shown to correspond reliably with MAP.
5. DBP value is associated with the point when oscillations level off.

The oscillation method can reliably determine only mean arterial pressure. SBP and DBP values are later estimated by using the empirical protocols, and often are less accurate than in auscultatory measures. SBP tends to be overestimated and DBP underestimated [18].

Occlusive methods of BP measurement are non-invasive and suitable for many clinical uses. To improve the performance and enable home monitoring, systems are automated, so that they do not require constant supervision and reduce error coming from human operator. Since huge errors may result from too slow/too fast cuff deflation, automatically operated cuffs has been developed, with electrical pump and valve. In auscultatory method e.g. the microphone can be used, replacing human ear. However, there are important drawbacks, that cannot be overcome. All occlusive methods are intermittent: single determination of BP can take entire minute to obtain

and the pause of 20 minutes between the measures is recommended, so that the circulation under cuff return to normal [24]. Therefore, short-term changes in BP cannot be detected. Furthermore, the inflation of the cuff always causes discomfort of the patient, which may produce pain and contribute to the patient's stress level. It results also in alterations of the BP. These problems are important e.g. when investigating BP fluctuations during sleep [14].

3.2.2. Volume clamp method

Currently the most commonly used continuously monitoring solution is volume clamp method, invented by Jan Peňáz in 1973 [26]. It requires using photoplethysmogram (PPG) sensor placed inside the transparent cuff, while the cuff is attached around the finger and connected to the pressure controller. Photoplethysmographic sensors enable measurement of blood volume alterations. The controller unit (servo mechanism) is used to adjust the cuff pressure, such that the blood volume in the finger will be constant. Then, the cuff pressure will represent the actual arterial pressure. The system automatically corrected changes induced by smooth muscle contractions or relaxations [27]. This technique is also known as a vascular unloading. Commercial adaptations of this solutions can be found in FinapresTM, FinometerTM and PortapresTM devices by Finapres Medical Systems.

Although the volume clamp enables continuous and non-invasive monitoring of BP with acceptable accuracy, it is also based on using a pneumatic cuff, which is causing the discomfort of the patient by constant press on the finger and can compromise the circulation. Peripheral vasomotor changes also cause error, primarily affecting systolic readings [28, 29]. If the cuff is applied incorrectly, calibration problems may occur, and no clearly defined method exists for determining the accuracy of cuff adjustment [30].

3.2.3. Tonometry

Applanation tonometry is a method introduced by Gerald Pressman and Peter Newgard in 1963. It consists of a probing element (transducer or rigid sensor array), which is attached on the skin above the pulsating artery, and an inflatable cuff. It can be used on any artery with a sufficient support of the bone, usually radial artery [27]. Setup measures blood pressure alterations by pressing (but not occluding) the artery against bone using a cuff. Skin and tissue transfer pressure pulsations to the probe. The vessel flattens when the pressure and, consequently, the force against the artery wall increases. The cuff pressure is adjusted to maintain the flattened shape of the artery, with the wall tension perpendicular to the probe [25]. Arterial pressure in the top of the flattened artery's center equals the supporting pressure, allowing the recording of a pressure waveform.

Although the relative shape of the tonometric waveform is generally considered similar to catheter, the absolute blood pressure is hard to determine and it has to be calibrated with initial BP values obtained using independent technique (e.g. cuff sphygmomanometry) [30]. Except of the calibration problems, errors can appear also due to difficulties with accurate and reproducible sensor positioning. Wrist movements and tendons are a source of artifacts and measurement inaccuracies. Another limitation of this method is its relatively high cost and the measurement of

the peripheral circulation, which has different pressures from more centrally-located sites (as described in Section 2.2.2).

3.2.4. Pulse Decomposition analysis

One of the attempts to non-invasive continuous blood pressure monitoring is Pulse Decomposition Analysis. It was introduced in a commercial system called CareTaker (Empirical Technologies Corporation, Charlottesville, Virginia). This solution consist of three basic components: a finger cuff that couples to an arterial pressure point, a pressure line that pneumatically telemeters the pulsations, and a piezo-electric pressure sensor that converts the pressure pulsations into a voltage signal [31]. The BP is detected with the Pulse Decomposition Analysis (PDA) algorithm from the voltage signal. PDAs premise is that the peripheral arterial pressure pulse is a superposition of five individual component pressure pulses that are due to the left ventricular ejection and reflections and re-reflections from only two reflection sites within the central arteries [32]. PDA principles are sketched in Figure 4:
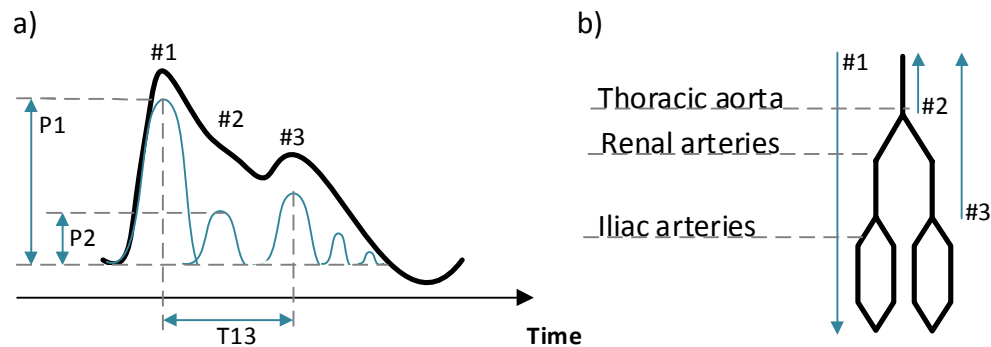

Figure 4. PDA principles: a) pulse components, b) reflection sites.

There are three component pulses of interest:
- primary pulse (P1), which originates directly from the left ventricular ejection,
- second systolic pulse (P2), that arrives subsequently to the primary pulse and originates at the junction between thoracic and abdominal aorta (renal reflection),
- tertiary pulse (P3), which is a reflection of the primary pulse that originates at the site where the abdominal aorta bifurcates into the iliac arteries [33].

In sufficiently long cardiac cycles two additional components (P4, P5) can be observed in the tail end of radial or digital arterial pulse [34].

The algorithm to calculate the BP consists of four components: a peak finder that identifies heartbeats in the data, a differentiator that produces the second derivative, an integrator that generates the integrated pulse wave form from which relative component pulse amplitudes are determined, and a low-pass filter that allows identification of the primary systolic peak. Once the locations of the reflection component pulses and the systolic peak are identified, the T13 interval is calculated. The T13 is the time delay between the systolic (P1) and the iliac (P3) peak. The P2/P1 ratio is calculated using the amplitudes of the P2 peak and the systolic peak, in the integrated pulse spectrum. The T13 and P2/P1 are important parameters in tracking the changes in BP [31].

3.2.5. *Pulse Transit Time and Pulse Wave Velocity*

Pulse Transit Time is the time between two pulse waves propagating on the same cardiac cycle from two separate arterial sites. It can be used to calculate Pulse Wave Velocity, since:

$$PWV = \frac{d}{PTT},$$

(2)

where is the distance between two measurement points. PWV has been widely used for the estimation of arterial stiffness and has been proposed for BP estimation as well. It is assumed that PTT is inversely related to BP, since with increasing BP, increasing distending pressure and decreasing arterial compliance, PWV rise and thus PTT shortens [35, 36].

Although in this method PTT cannot be used for the measurement of BP absolute values, its short-term changes can be estimated [35, 37-39]. Commonly, such measurements are performed by using electrocardiography (ECG) and photoplethysmography (PPG) signal, which is usually measured from the fingertip (Figure 5). However, the PTT can be measured also using other sensors and sensor placements.
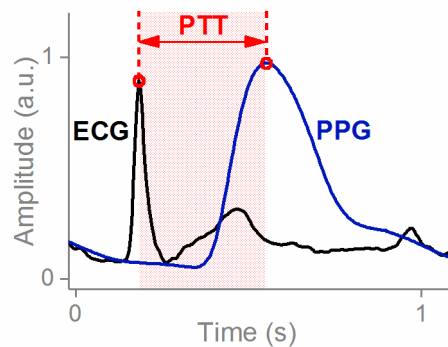

Figure 5. Measuring PTT using ECG and PPG sensors.

PWV-based technique provides the best trade-off between clinical and ambulatory compliances [24]. It would be fully exploited, if PWV would be measured along central elastic arteries, where no vasomotion phenomenon exists. In method tested in this study attempts are to obtain PWV of central arteries, which would benefit in the development of a noninvasive and non-occlusive BP measurement technique.

4. METHOD OF MEASUREMENT AND SIGNAL ANALYSIS

4.1. PTT measurement utilizing optomechanical accelerometers

In this study, PTT measurement was performed using optomechanical accelerometers (ACMs) [10, 40, 41] This technique was developed by researchers from Optoelectronics and Measurement Techniques research unit (University of Oulu) as a part of a multimodal setup, which enables monitoring of various physiological functions simultaneously and in non-invasive manner. Aim of this setup is to observe, how physiological functions are connected to brain activity. Existing cuff-based methods are not suitable for long-term monitoring, as described in Section 3.2.1. However, in the correlation analysis of physiological signals, of interest are fluctuations of the signals and different variables rather than the absolute values. Thus, continuous measure of oscillations of BP is sufficient, which can be done using ACMs and PTT method (Section 3.2.5).

4.1.1. Hardware

The ACM sensor consists of two static optical fibers: one serving as a light source and the other as a light sensor. Fibers are attached to a cantilever and light is aimed at the free end of the cantilever [10]. Fibers are placed in a PolyOxyMethylene plastic box that measures 41 mm x 28 mm x 15 mm. Cantilever is made of brass foil, and its size is 18 mm x 5 mm x 0.05 mm. Sensors scheme is shown on Figure 6:
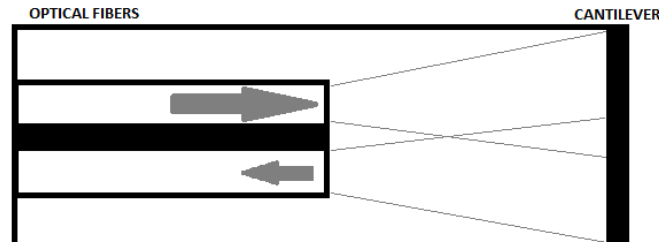

Figure 6. ACM sensor with two optical fibers at the left side and the cantilever on the right side.

At each heartbeat, blood is forced through the peripheral vessels, constantly changing their diameter. This corresponds to tiny movements of the skin, especially near the arteries. ACM sensor is attached tightly to the skin and the acceleration caused by the heartbeat bends the cantilever. Deformation of the cantilever causes a deflection of the beam, which changes the amount of reflected light. The output voltage is proportional to the intensity of the reflected light. As no mirrors or prisms are required, the structure of the sensor is simple and affordable.

Expected bandwidth of interest is between 15 Hz and 35 Hz [10]. Resonance frequency of the fabricated ACM is equal to 58Hz, which is sufficiently high for the application, since it should be well above this bandwidth.

4.1.2. Measurement method

ACMs are placed on the chest and on the neck of the patient. They are sensitive to blood pulsation and thus enable to estimate heart rate and transit time between pulse appearances in these two placements (Figure 7).
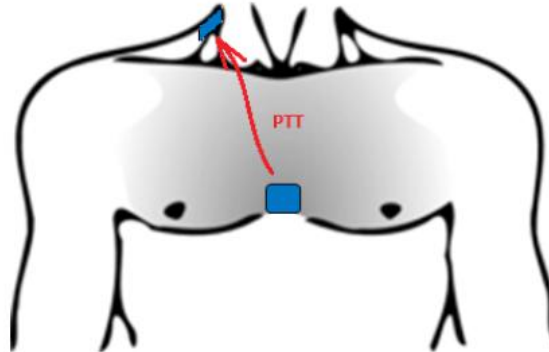

Figure 7. ACM sensor placement.

 The relationship between PTT, PWV and BP has been described in Section 3.2.5 Because of placing both sensors in the central part of the body, a common problem of measuring peripheral BP values is avoided (see Section 2.2.2).

Sampling frequency used for ACM signals is 10kHz. Signals are stored in multiple .lvm files, each file containing consequent part of the recording. .lvm files can be directly imported to MATLAB.

4.2. Signal analysis

Signal processing procedures were performed using MATLAB Mathworks software.

4.2.1. ACM signal filtering

As it was described in Section 4.1.1, raw ACM signal consists of heartbeat acceleration frequency components (between 15 and 35 Hz) and sensor's resonance frequency at 58Hz. During the recording with IBP (Test I, Section 5.1.1), raw signals were automatically filtered by LabView software, and thus available signals were already limited to the bandwidth of interest. However, during the recording with Finometer (Test II, Section 5.2.1) full bandwidth was recorded. In this case, in order to enable precise peak detection for every heartbeat, raw signal was bandpass-filtered with Butterworth filter of bandwidth 15Hz – 35 Hz. Magnitude response of a filter is shown on Figure 8:
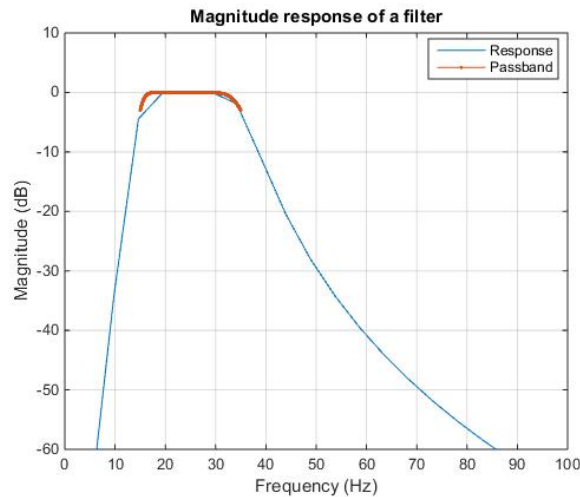
Figure 8. Magnitude response of a Butterworth filter used to filter ACM signals during Test II.

Single cardiac cycle before and after filtering is shown on Figure 9 (left). Spectra of these sequences are shown on the right.
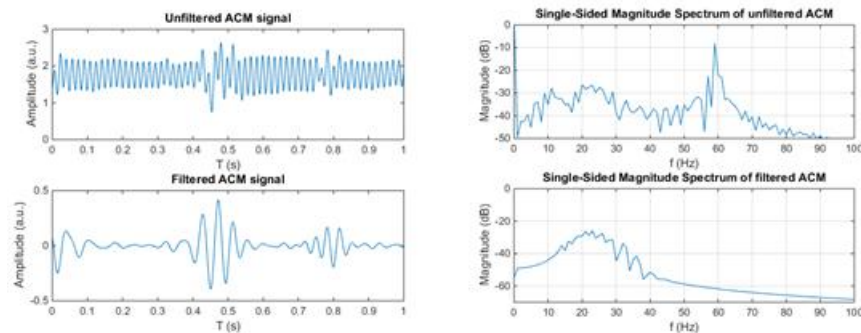

Figure 9. One cardiac cycle detected by ACM1 sensor and corresponding spectrum: unfiltered signal (top), band-pass filtered signal (bottom)

4.2.2. ACM peak detection

To calculate PTT between pulses detected in two locations, it is necessary to determine exact time of systolic peak appearance in both locations. ACM sensors are placed relatively close to each other; thus, it is important to achieve proper accuracy. For each cardiac cycle, sensors detect two pulsations (systolic and diastolic) which have almost similar shape. Diastolic peak usually has smaller amplitude, but it would be anyway detected as a local minimum. Thus, at the first step of peak detection, the matched filtering was used.

At the beginning of the filtering, part of the signal serving as a template must be defined. Template should include systolic peak and diastolic peak, as shown on Figure 10. In order to achieve better accuracy, template was chosen individually for each set of data.
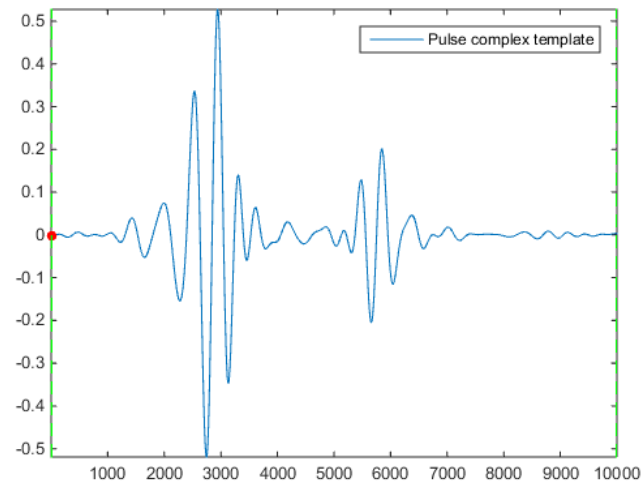
Figure 10. Pulse complex template, used as an input of matched filter.

The impulse response of the matched filter is derived from the template selected. The output of the filter (Figure 11b) shows maximum values when the beginning of a complex was detected (Figure 11a).
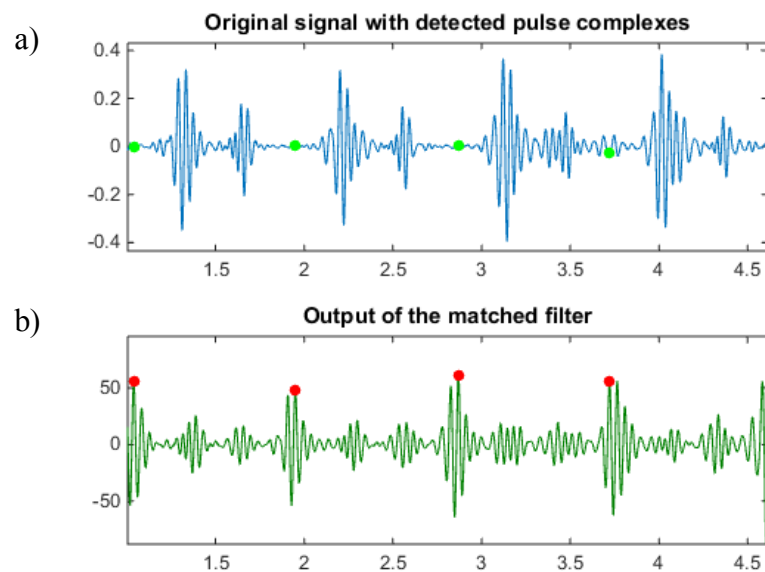

Figure 11. The result of matched filtering: beginning of each detected complex (green marker, a)), output of the filter with maximum values when the beginning of a complex was detected (red markers, b)).

When each cardiac cycle was found, it is easy to find local maxima/minima within fixed time window with proper thresholding. Figure 12 shows four cardiac cycles detected in ACM signal. Red markers shows the moment of opening of the aortic valve [10].
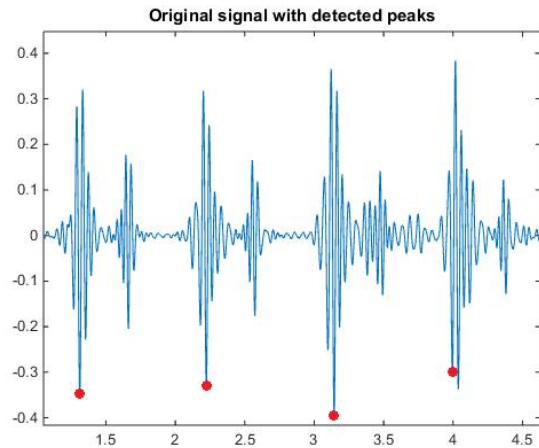
Figure 12. ACM signal with detected systolic peaks.

Heart rate was calculated for each signal, since it helps to detect errors and other abnormalities. On Figure 13 HR calculated using heartbeats detected in ACM signal is presented. Signal was recorded during breath holding task and it is clearly visible how HR drops at the beginning of each breath holding phase.
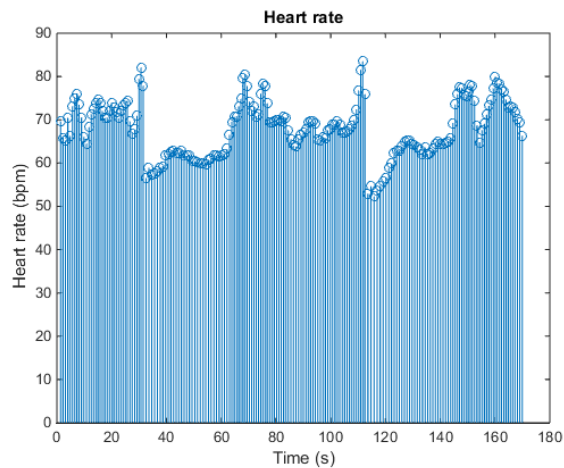

Figure 13. HR calculated using heartbeats detected in ACM signal.

4.2.3. *Peak detection in signal recorded by Finometer and IBP*

Due to the clear structure of signals recorded by both Finometer and IBP, the peak detection algorithm was rather straightforward. In these signals, at first all local maxima were founded and then filtered using amplitude thresholding. Maxima detected for each cardiac cycle gave direct information on SBP. Two cardiac cycles detected in Finometer signal are shown on Figure 14, with systolic peaks marked with red dots.
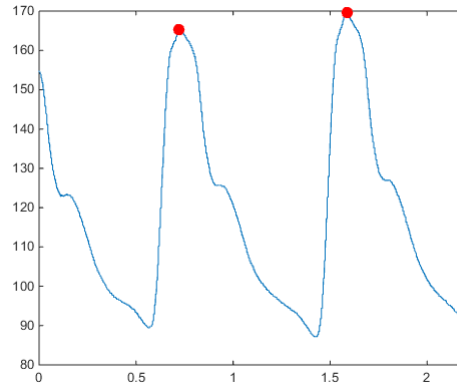
Figure 14. Finometer signal with detected systolic peaks.

With the information about consequent peaks timing it was possible to calculate heart rate, which was later compared with ACM heart rate.

4.2.4. Pulse Transit Time calculation

Signal from the neck (ACM2) was more vulnerable to be corrupted with noise, because the sensor was placed on soft tissue and might record skin vibrations not connected to blood pulsations. Second sensor placement – on the sternum (ACM1) - is more rigid. Thus, ACM1 was chosen to be treated as a reference.

   To calculate PTT value, peaks in ACM2 signal corresponding to systolic peaks detected in ACM1 were founded by defining proper time window, as shown on Figure 15:
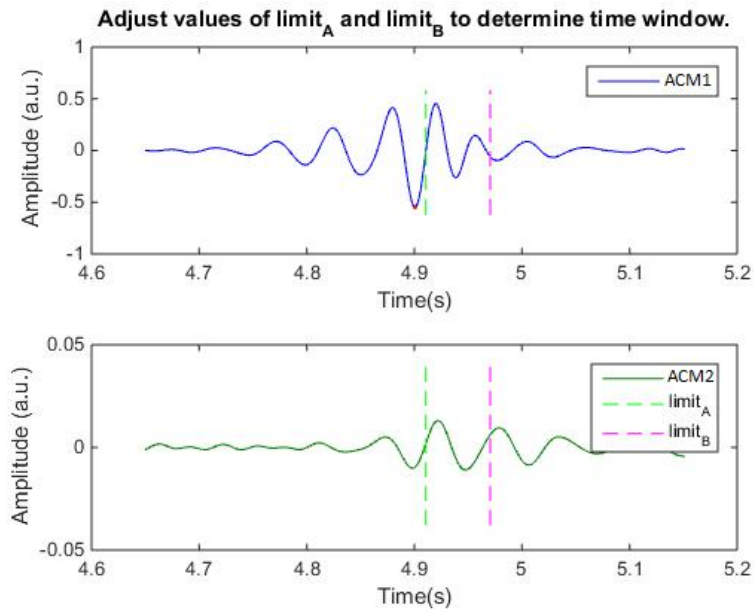

Figure 15. ACM1 and window for searching corresponding systolic peak in ACM2.

4.3. Data analysis and statistical methods

One of the challenges of the PTT- based method is modelling of the relation between measured PTT values and corresponding BP levels. In this study, three approaches to the problem were tested. Models are described in Section 4.3.1. Evaluation of models' performance was done using tools described in Section 4.3.2.

4.3.1. PTT-BP conversion models

Three mathematical models of converting PTT to BP were tested:

Model I: Linear regression

Relation between PTT and BP was modeled using standard linear regression to fit a linear function [11]:

$$y = ax + b,$$
(3)

In the analyzed case, the function was expressed as:

$$BP_1 = a \cdot PTT + b,$$
(4)

Model coefficients were found using a least-squares fit. Data pairs for each patient were modeled individually.

Model II: Non-linear Moens and Korteweg model

In 1878 Moens and Korteweg derived a mathematical expression for the velocity of the pulse front traveling along an artery as a function of vessel and fluid characteristics [12, 13]:

$$PWV = \sqrt{\frac{h \cdot E}{2 \cdot r_0 \cdot \rho}},$$
(5)

Where PWV – pulse wave velocity, ρ is the blood density, r_0 is the inner radius of the vessel, h is the vessel wall thickness, and E stands for Young's modulus describing the elasticity of the arterial wall. Young's modulus E is not a constant, but it is pressure-dependent. The relationship is of the form:

$$E = E_0 \cdot e^{\alpha \cdot P},$$
(6)

where E_0 is the zero pressure modulus, α is a constant that depends on the vessel and P is pressure. Thus, relation between PWV and BP can be expressed as:

$$PWV = \sqrt{\frac{h \cdot E_0 \cdot e^{\alpha \cdot BP}}{2 \cdot r_0 \cdot \rho}},$$
(7)

Thus:

$$BP = \frac{1}{\alpha} \cdot \ln\left(\frac{2 \cdot r_0 \cdot \rho \cdot (PWV)^2}{h \cdot E_0}\right), \tag{8}$$

As explained in Section 3.2.5, PWV is defined as:

$$PWV = \frac{d}{PTT}, \tag{9}$$

where d is the distance between two measurement points. It can be assumed that d and E_0 remains constant and that ρ, r, and h show only small changes [42], and following the method shown in [10], the relation can be expressed as:

$$BP_2 = \frac{1}{\alpha} \cdot \ln\left((\frac{d}{PTT})^2\right) + \frac{1}{\alpha} \cdot \ln\left(\frac{2 \cdot r \cdot \rho}{h \cdot E_0}\right) = k_2 - k_1 \cdot \ln\left(PTT^2\right), \tag{10}$$

Model III: Nonlinear model by Gesche et.al

3rd approach tested in this study was model presented in 2012 by Heiko Gesche et.al. [14]. In this model, PTT to BP conversion is quasi-linear for low BP values, but increase exponentially at higher pressures. Main function used in this model is:

$$BP_3 = \overset{I}{\left\{m_1 \cdot PWV \cdot e^{(m_2 \cdot PWV)}\right\}} + \overset{II}{\left\{m_3 \cdot PWV^{m_4}\right\}} - \overset{III}{\left\{m_5\right\}}, \tag{11}$$

Parameters m_1–m_5 were estimated using least-square method. Segments I and II were analyzed separately, then they were added and segment III was searched. PWV was defined by formula (9), with the distance d arbitrarly defined as 20 cm.

4.3.2. *Analysis tools*

In all three tests, data pairs for each patient were modeled individually. Obtained results were compared with reference BP values using Pearson's correlation coefficient and Bland – Altman plot. These tools were chosen due to its common use in the literature in the field of NIBP measurements.

Pearson's correlation coefficient is used to measure linear dependence between two values. It is suitable for the experiment presented in this study, since the errors effecting from improper initial BP level do not affect the result of comparison. The significance level used in this study was $p<0.005$.

Second tool used for comparison was Bland-Altman plot. In this method, the mean value calculated from corresponding BP values obtained from both methods is plotted against the corresponding difference of the mean BP minus the BP_{ACM}. The agreement limits were defined by mean $\pm$ 1.96 of the standard deviation (SD) of the differences. This graphical representation helps to assess the disagreement between the two measures.

5.   RESULTS

To evaluate the three BP estimation models it was necessary to conduct measurements with the reference method. Standard occlusion methods are easily accessible, but the BP value is measured only once in few minutes and thus it was insufficient in this study. However, it was possible to obtain BP values measured using two reference techniques. One group of measurement session included invasive method of measuring BP (IBP, see Section 3.1) recorded simultaneously with ACM signals. Second group of sessions included monitoring with commercial device: Finometer™ (FMS, Finapres Measurement Systems, Arnhem, Netherlands), which is utilizing volume-clamp method measurement method (see Section 3.2.2). These measurements were also simultaneous with ACM recording.

5.1.   Test I: Comparison with invasive BP measurement

IBP data used in this section are part of the study run by researchers from OPEM unit (University of Oulu) and OFNI group (Oulu University Hospital). Data were collected in 2014 during the blood-brain barrier disruption (BBBD) procedure, which was conducted at the Oulu University Hospital. Prior to the procedure, each patient signed an informed consent to use the data for study and research purposes. The study was carried out in accordance with the Declaration of Helsinki and approved by the Ethical Committee of Northern Ostrobothnia Hospital District, Oulu University Hospital (number 5/2014).

5.1.1.   Measurements

Eight sets of ACM and IBP data are used in this study, collected during separate procedures from four different patients. Information about patients' characteristics, is shown in Table 2:

Table 2. Patients' characteristics

#	Gender M/F	Age
1	M	61
2		
3		
4		
5	F	20
6	M	64
7		
8	F	68

ACM sensors were placed on patient's chest (ACM1) and neck (ACM2). IBP signal was measured by intra-arterial catheter, placed in femoral artery (Figure 16).
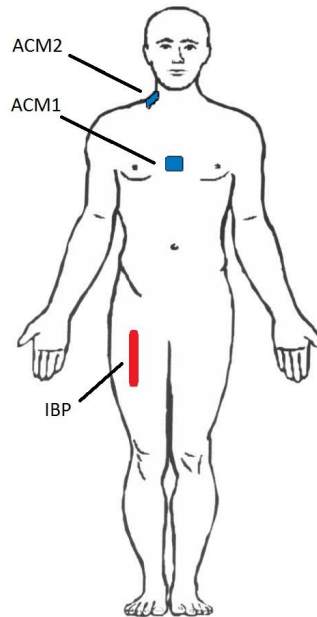
Figure 16. ACM and IBP sensor placement.

Results for each method were recorded using separate system, and thus manual synchronization was needed for all of the measurements. ACM signals were recorded with sampling frequency equal to 10kHz, while IBP signals were recorded using commercial device with sampling frequency 300 Hz.

5.1.2. Results

HR was used as an indicator of proper synchronization and correct peak detection. It was assumed that high correlation between HRs means that corresponding peaks in signals were founded correctly. Pearson's correlation coefficients between HR measured by ACM chest sensor (HR_{ACM1}) and intra-arterial catheter (HR_{IBP}), and between HR measured by ACM chest sensor (HR_{ACM1}), and ACM neck sensor (HR_{ACM2}) were calculated for each measurement. Results are shown in Table 3:

Table 3. Pearson's correlation coefficients between HRs.

#	Pearson's r coefficient	
	HR_{ACM1}, HR_{IBP}	HR_{ACM1}, HR_{ACM-2}
1	0.79	0.97
2	0.58	0.99
3	0.83	0.97
4	0.56	0.98
5	0.85	0.75
6	0.78	0.95
7	0.48	0.99
8	0.59	0.93
Average	0.6825	0.94125

One of the challenges of data analysis in Test I was lack of automatic signal synchronization and huge difference between sampling frequency in compared

measurements. Visual inspection was made in order to set possible delay between signals with maximum accuracy. After that, correlation function was calculated to set a definite level of delay. Thus, values presented in Table 3 are maximum correlation coefficient that was possible to achieve. For a comparison between HR_{ACM1} and HR_{IBP} these values vary between 0.48 and 0.85. Low correlation might be an effect of different sampling frequencies and/or errors in ACM peak detection, since this signal is very vulnerable to artifacts. It must be noted that incorrect peak finding in ACM signal result in decrease of BP estimation.

Example of measured HR signals using separate sensors is shown on Figure 17:
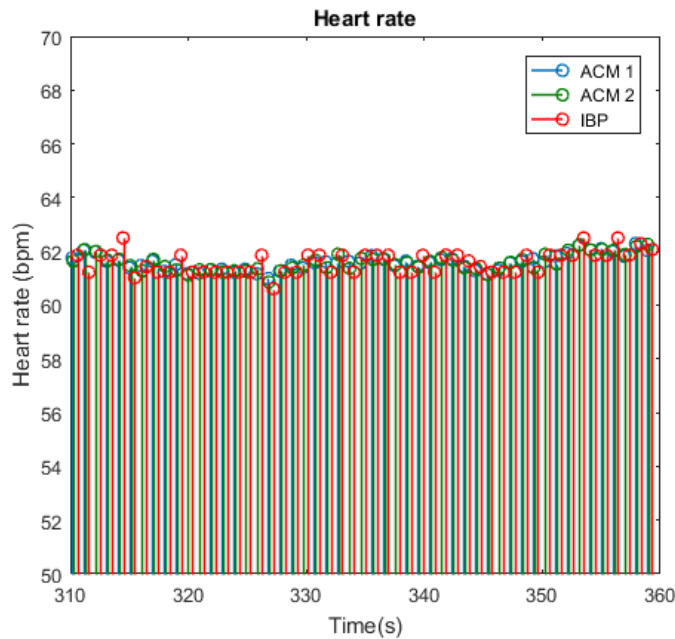

Figure 17. HR detected with ACM1, ACM2 and IBP during measurement 3.

PTT was calculated between heartbeats detected using ACM1 and ACM2. Then, it was used for BP estimation. Because of possible influence of motion artefacts. physiological differences between 2 arterial sites and peak detection errors, PTT signal and corresponding BP_{IBP} curve were smoothed using 3rd order Savitzky-Golay filter (SG), with frame length 51. Example of raw PTT data with corresponding smoothed curve are shown on Figure 18:
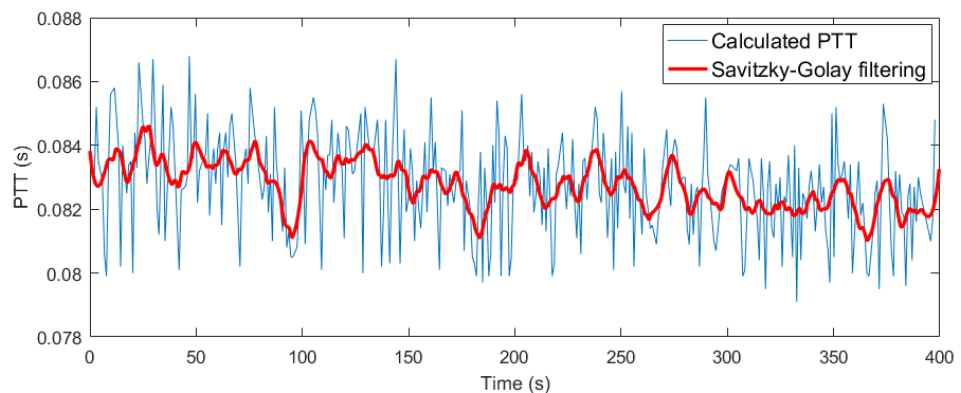

Figure 18. Raw PTT data and SG smoothed curve, measurement 5.

PTT signal was used to estimate level of SBP using three mathematical models, as described in Section 4.3. Pearson's correlation coefficient between estimated values

and corresponding invasively measured BP (BP_I) was calculated separately for raw data and SG smoothed data. Results for linear regression model (BP_{LIN}), non-linear model based on Moens and Korteweg publication (BP_{M-K}) and nonlinear model presented by Gesche (BP_G) are shown in Table 4:

Table 4. Pearson's correlation ceofficients between tested models and BP_I.

#	Signal length (s)	Number of data pairs	Pearson's r coefficient					
			BP_{LIN}		BP_{M-K}		BP_G	
			raw	SG	raw	SG	raw	SG
1	100	77	0.39	0.65	0.4	0.65	0.4	0.65
2	100	33	0.42	0.68	0.42	0.68	0.42	0.68
3	400	356	0.32	0.64	0.31	0.64	0.31	0.64
4	100	82	0.37	0.54	0.37	0.54	0.37	0.54
5	600	616	0.49	0.59	0.49	0.6	0.46	0.6
6	200	76	0.26	0.39	0.26	0.39	0.26	0.39
7	600	345	0.47	0.51	0.47	0.51	0.47	0.51
8	100	59	0.44	0.43	0.45	0.44	0.45	0.44
Average	275	205.5	0.4	0,55	0.4	0.56	0.39	0.56

Because of motion artifacts, present especially in ACM2 signal not every pulse complex could be distinguished, e.g. in measurement 6 the signal had duration of 200 seconds, but only 76 pulse complexes were found. Although pulse complexes used for PTT calculation in measurement 6 passed the selection, resulting correlation with reference BP is still rather low for all tested models.

Model coefficients were founded separately for each of eight individual data sets using least-squares method. Resulting best-fit curves are shown on Figure 19,
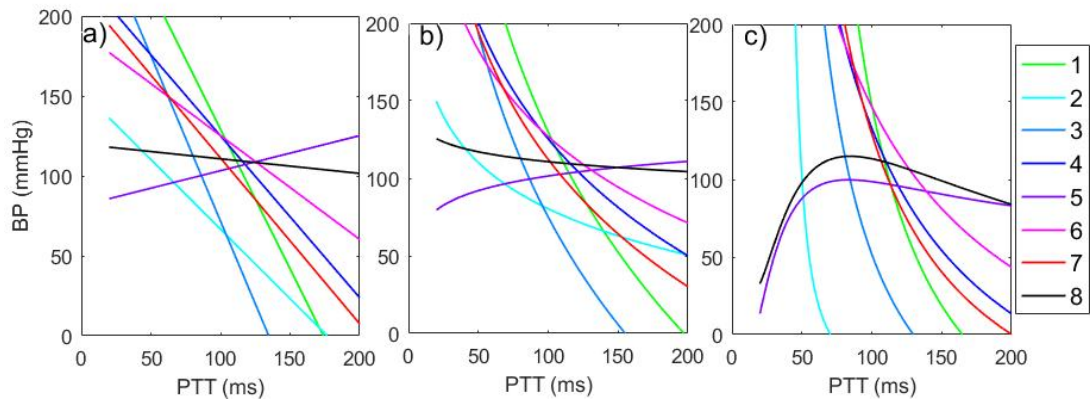

Figure 19. Best-fit curves generated for tested models: linear regression(a), non-linear Moens - Korteweg model (b), non-linear Gesche model (c).

Example of estimated BP values using tested models and corresponding BPI signal is shown on Figure 20:
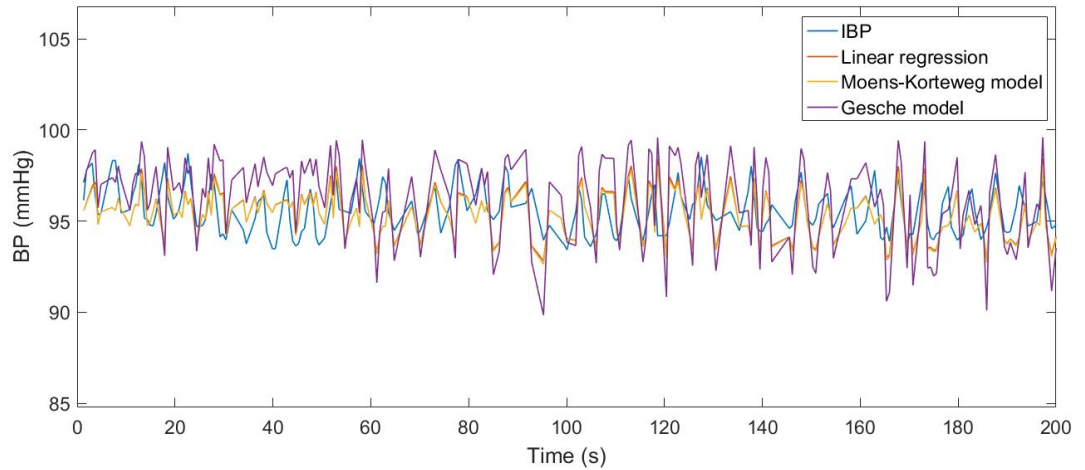
Figure 20. BP measured using IBP and estimated using PTT and three mathematical models (measurement 5).

Bland-Altman analysis was performed for all three models. Resulting coefficients of reproducibility are presented in Table 5:

Table 5. Bland- Altman's coefficient of reproducibility for 3 tested models

#	Coefficient of reproducibility (mmHg)		
	BP_{LIN}	BP_{M-K}	BP_G
1	6.06	6.06	9.74
2	3.55	3.55	4.02
3	6.73	6.74	12.00
4	4.32	4.33	6.36
5	2.76	2.76	4.44
6	3.46	3.45	4.53
7	5.55	5.56	8.03
8	3.80	3.78	5.40
Average	4.53	4.53	6.81

Example of Bland-Altman plots obtained for one data sets using three models is shown on Figure 21:
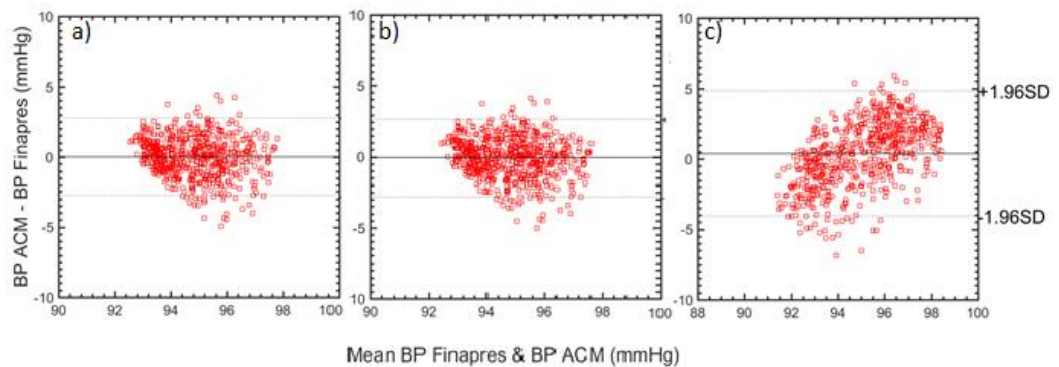

Figure 21. Bland-Altman plots generated for measurement 5 using tested models: linear regression(a), non-linear Moens - Korteweg model (b), non-linear Gesche model (c).

All three models showed comparable results. Pearson's correlation coefficients in Test I varied between 0.26 and 0.49 for raw data and between 0.39 to 0.68 for SG smoothed curves. It is surprisingly low result, although for Bland – Altman analysis coefficients of reproducibility were much more promising: 2.76 – 6.73 mmHg for linear model, 2.76 – 6.74 mmHg for Moens -Korteweg model and 4.02 – 12 mmHg for Gesche model. It is interesting how complex Gesche model do not show significant improvement in correlation coefficient r, with actually much poorer performance in Bland – Altman analysis, when compared to other, much simple models.

5.2. Test II: comparison with volume-clamp method

In second part of the study BP serving as a reference was measured using volume-clamp method, utilized in commercially available Finometer™ (FMS, Finapres Measurement Systems, Arnhem, Netherlands).

5.2.1. Measurements

Measurements described in this section were conducted in Oulu University Hospital. There was only one, healthy subject, performing five different tasks. Tasks were selected due to their influence on blood pressure. In each task subject was lying flat on the bed. Sensors placement is shown on Figure 22:
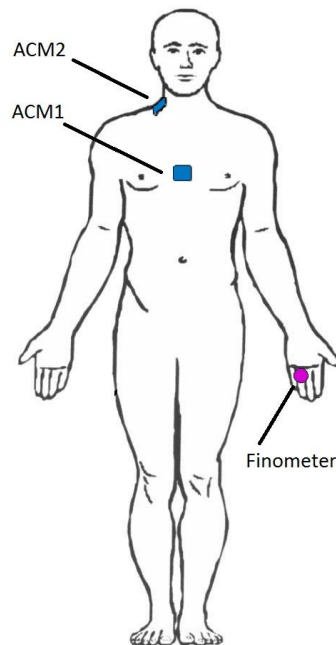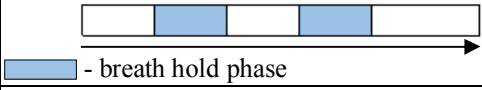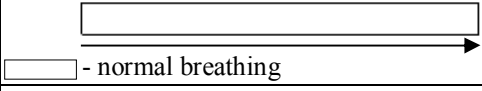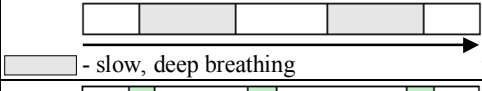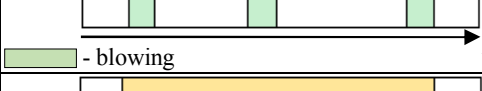

Figure 22. ACM and Finometer sensor placement.

Both ACM signals and BP measured using Finometer (BP_{FIN}) were recorded with sampling frequency equal to 10kHz. They were recorded in synchrony and together with other modalities visualized by Lab View software.

List of performed tasks and scheme of every task are shown in Table 6:

Table 6. List of tasks performed during the measurement session.

#	Task	Duration (s)	Scheme
1	Breath-hold	170	
2	Resting state	700	
3	Deep breathing	240	
4	Blowing	270	
5	Tilt	550	

5.2.2. Results

Pearson's correlation coefficients between HR measured by ACM chest sensor (HR_{ACM1}) and Finometer (HR_{FIN}), and between HR measured by ACM chest sensor (HR_{ACM1}), and ACM neck sensor (HR_{ACM2}) were calculated for each measurement. Results are shown in Table 7:

Table 7. Pearson's correlation coefficients between HRs.

#	Pearson's r coefficient	
	HR_{ACM1}, HR_{FIN}	HR_{ACM1}, HR_{ACM-2}
1	0.98	0.99
2	0.94	0.99
3	0.98	0.99
4	0.95	0.99
5	0.91	0.98
Average	0.952	0.988

In HRs comparison made for Test II, the output correlation coefficients meet expectations – for all tasks, its value exceeds 0.9, which is an excellent result. HR signals detected during Task 3 using separate sensors is shown on Figure 23. Deep breathing phase can be clearly distinguished.
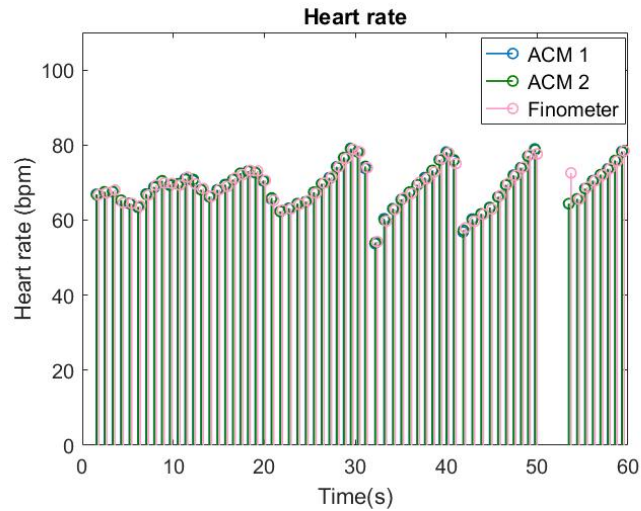
Figure 23. HR detected with ACM1, ACM2 and Finometer during Task 3.

PTT signal and corresponding BP_{FIN} curve were smoothed using 3rd order Savitzky-Golay filter (SG), with frame length 51. Example of raw PTT data with corresponding smoothed curve are shown on Figure 24:
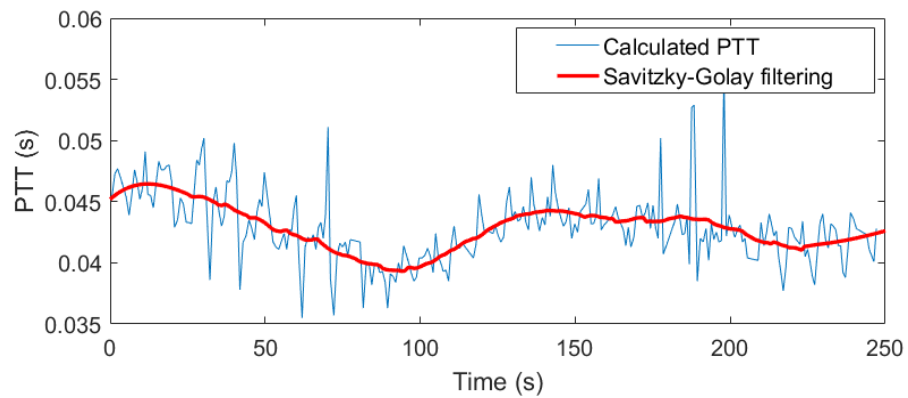

Figure 24. Raw PTT data and SG smoothed curve, Task 3.

Similarly as shown in Section 5.1.2, PTT signal was used to estimate level of SBP using three mathematical models. Pearson's correlation coefficient between estimated values and corresponding BP measured by Finometer (BP_{FIN}) was calculated separately for raw data and SG smoothed data. Results for linear regression model (BP_{LIN}), non-linear model based on Moens and Korteweg publication (BP_{M-K}) and nonlinear model presented by Gesche (BP_G) are shown in Table 8:

Table 8. Pearson's correlation coefficients between tested models and BP_{FIN}.

#	Signal length (s)	Number of data pairs	Pearson's r coefficient					
			BP_{LIN}		BP_{M-K}		BP_G	
			raw	SG	raw	SG	raw	SG
1	170	174	0.31	0.62	0.31	0.61	0.32	0.61
2	700	692	0.3	0.43	0.3	0.44	0.31	0.44
3	250	268	0.25	0.6	0.24	0.6	0.21	0.59
4	260	245	0.13	0.46	0.14	0.46	0.12	0.45
5	600	539	0.23	0.48	0.22	0.48	0.22	0.45
Average	396	383.6	0.24	0.52	0.24	0.52	0.24	0.51

Model coefficients were founded separately for each of eight individual data sets using least-squares method. Resulting best-fit curves are shown on Figure 25:
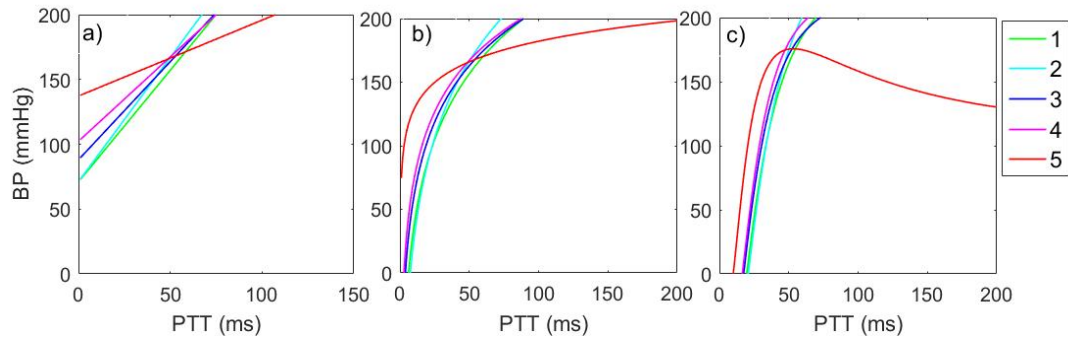

Figure 25. Best-fit curves generated for tested models: linear regression(a), non-linear Moens - Korteweg model (b), non-linear Gesche model (c).

Analysis of best-fit curves (Figure 19, Figure 25) might help to interpreted similarities between results given by different models. It can be observed, that despite of non-linear nature of models II and III, in the scope of obtained PTT values the model is basically linear. Non-linearities are more significant for Test II, however, the curves orientation in this test reveal positive relationship between PTT and BP. It is not only opposite to the results from Task I, but also contrary to the theories presented in professional literature.

BP values estimated during Task 3 using tested models and corresponding BP_{FIN} signal is shown on Figure 26. Deep breathing phase is characterized by higher BP amplitude changes.
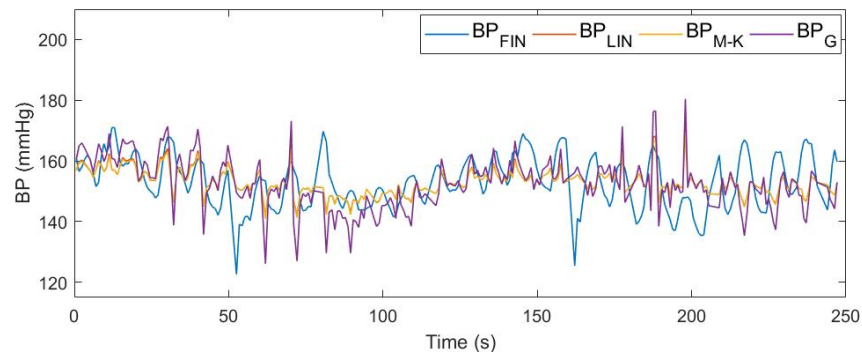
Figure 26. BP measured using Finometer and estimated using PTT and three mathematical models (Task 3).

Bland-Altman analysis was performed for all three models. Resulting coefficients of reproducibility are presented in Table 9:

Table 9. Bland- Altman's coefficient of reproducibility for 3 tested models

#	Coefficient of reproducibility (mmHg)		
	BP_{LIN}	BP_{M-K}	BP_G
1	19.6	19.4	25.66
2	16.71	16.65	20.61
3	16.78	16.81	20.69
4	30.03	30.06	34.05
5	17.18	17.58	32.57
Average	20.06	20.1	26.72

Example of Bland-Altman plots obtained for one data sets using three models is shown on Figure 27:
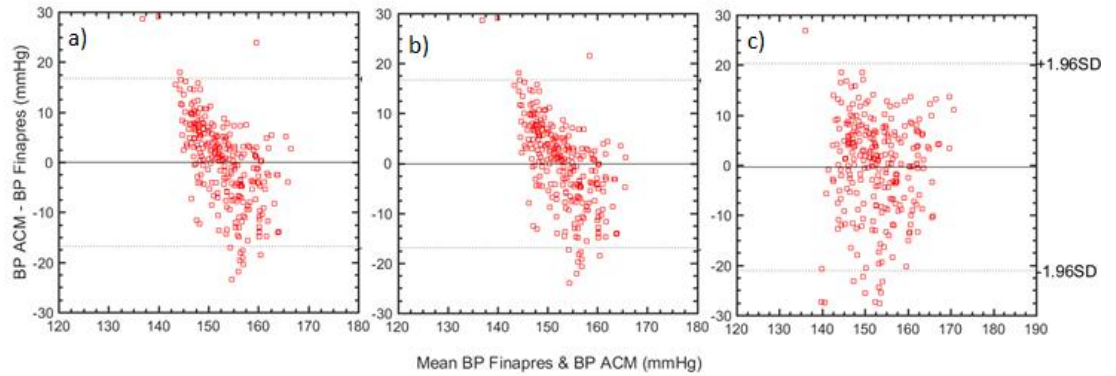
Figure 27. Bland-Altman plots generated for Task 3 using tested models: linear regression(a), non-linear Moens - Korteweg model (b), non-linear Gesche model (c).

In Test II, all models show comparable correlation rate (0.13 to 32 for raw signals, 0.43 to 62 for SG smoothed signals), followed by poor levels of reproducibility coefficients: 16.71 – 30.03 mmHg for linear model, 16.65 – 30.06 mmHg for Moens – Korteweg model and 20.61 – 34.05 mmHg for Gesche model.

6.   DISCUSSION

Presented study shows that BP can be estimated from PTT using three calculation models. Measurements were performed using two fiber optics based accelerometers. Similar studies have been most commonly conducted using PPG and ECG sensors used for PTT estimation [35, 43], and compared to BP measured by sphygmomanometry [14, 44]. In this study the emphasis was placed on testing PTT-based method for continuous, noninvasive and cuffless BP recording. Fiber optics based accelerometers were developed in University of Oulu and one of their biggest advantages is that they are fully compatible with other measurement techniques, in particular, MRI and MEG, and do not require ECG measurement which can have also limitations related to PTT measurements [40, 41]. This quality was already used in several published studies, [3, 10], in which ACMs were a part of multimodal setup.

In the related literature, the relation between PTT and BP was often reported as linear [11, 35], although in a number of publications also more complex approaches were developed [14]. In this study, three methods of BP-PTT relation modeling were tested: linear regression, non-linear Moens and Korteweg model and non-linear model by Gesche et.al. There were two sets of measurement data: one set was recorded simultaneously with invasively measured BP (Test I), and the other with Finometer (Test II). IBP and Finometer data were used as a reference, and comparison of the tested method was made by calculating Pearson's correlation coefficient and Bland-Altman analysis.

It must be noted that in order to eventually validate the accuracy of the technique, it is necessary to improve the quality of recorded signals. Although it is possible to do part of the work in post-processing, lot of the improvements could be in fact applied during data collection. Data sets in Test I were collected in 2014 and at the time no automatic synchronization between the signals were used, and thus the manual synchronization in post-processing was needed. Undoubtedly, this solution is not only time consuming, but also susceptible to errors. In addition, signals from ACM2 were rather poor quality for the entire Test I data sets. During every measurement signal from ACM2 is much more vulnerable for noise than ACM1, since it is often transmitting skin vibration, as the neck is a softer spot than thorax. Thus, ACM2 sensor require very careful attachment, which would ensure the heartbeat response with the highest amplitude. This however, was not possible during the Test I. Most probable cause was some kind of fiber damage, and although later both fiber and sensor were replaced, measurements dedicated for this study could not be repeated.

Results of the Test I and Test II are shown in Section 5.1.2 and Section 5.2.2 respectively. It was expected, that non-linear models would give results much more consistent with reference values. Surprisingly, both correlation test and Bland-Altman analysis gave opposite outcome, with the best score coming from linear model results. Nevertheless, in this study differences between models appear to be relatively small. One reason of that could be limited variation of BP values, which prevent of showing full spectrum of BP-PTT dependency for each subject. In Test II, breathing tasks were used to induce change of BP, however, in few tasks it resulted also in motion artifacts. It must be taken into account that there are significant limitations of linear model, since it might assume negative PTT values for very high BP as negative BP at higher PTT levels [35]. Despite of these drawbacks, linear

model can be considered as suitable if border BP values are not expected and if complicated, multi-point calibration is not possible.

Another result, which did not fully meet the expectations, is the orientation of best-fit curves. Despite of the theoretical assumptions, two curves from Test I and all five curves from Test II suggest positive relation between BP and PTT. In case of Test I it might be considered as an error of different sources, e.g. patient might receive vasoactive drugs before the measurement log has been started. It is also possible that despite of the highest carefulness during the manual signal synchronization, some sort of time lag was left and the signals are shifted, which would also explain slightly lower correlation between HR_{ACM1} and HR_{IBP} (average r=0.68) than between HR_{ACM1} and HR_{ACM2} (average r=0.94), see Table 3. Regarding Test II, positive orientation of best-fit curves is difficult to explain, especially when taking into account automatic synchronization of signals, excellent correlation of HRs (Table 7) and satisfactory overall signal quality. Additional experiments should definitely be performed in order to study the relation between PTT and BP. It might be important to induce BP changes otherwise than by breathing tasks, e.g. experiments with cold pressor test might be done. In the results presented in Test II, one subject performed all the tasks. Thus, huge similarity between the best-fit curves is of great value, since it suggests that in the future one calibration procedure will be enough to estimate model coefficients for each subject. Curve for the last task is slightly different, since in this task ('Tilt') whole body position has changed. It naturally suggests that the influence of body position on PTT should be thoroughly investigated.

It is also important to emphasize, how different were reference methods in Test I and Test II, regarding sensor type and placement. Since BP measurement with the catheter can be considered as a golden standard in BP measurement, consistence in Bland – Altman plot with relatively low coefficient of reproducibility in Test I might serve as a proof of PTT-based methods usefulness, despite of the lower accuracy when comparing to Finometer. It should be noted how different types of error can be seen in both tests. Bland – Altman plot for Test I (Figure 21) reveals that Gesche's model gives slightly underestimated values for lower mean BP values, as well as slightly overestimated values of BP for higher mean BP (positive trend). Other models do not have such clear trend and for all mean BP values we can see stable level of reproducibility coefficient. However, in Test II, analysis of Bland – Altman plot (Figure 27) results in different conclusions. Although trend for Gesche's model remains positive, both linear regression, non-linear Moens and Korteweg model have strong negative trend. Together with high coefficient of reproducibility, it results in a huge dispersion of the errors. High level of error is rather unforeseen, since the comparison of the predicted BP with the reference curve seem to be rather satisfactory for the bare eye (Figure 26). Nevertheless, in Test II some level of discrepancies between results could have been expected, since the Finometer sensor was placed on the distant finger artery, whereas PTT was measured on the torso.

In order to improve the technique it is necessary to plan further hardware and software improvements, followed by validation of the results. Thus, observations presented in Test I in this study will be taken into account when planning the measurements and during later data analysis. NIBP hardware is also constantly being improved, and in future measurements the signal quality will be automatically checked and signalized immediately after sensor attachment. Such solution will be highly beneficial, since recording the data with the ICU patients is time consuming and difficult to organize, and it is important to use this unique possibility to its best

without the risk of recording poor quality data. In the future, it will be also useful to improve filtering and peak detection, so that the system will be faster and more automated, without the need of constant manual control. It would also open the way to create real-time monitoring system, with all the benefits of such solution.

At present, the biggest advantage of the presented NIBP technique is its compatibility with other modalities and ability to work continuously and non-invasively. It encourages using the setup for research purposes, especially during brain studies utilizing MRI or MEG. Several studies applying ACMs have already been conducted, e.g. in [3] ACMs were used simultaneously with near-infrared spectroscopy (NIRS) and MEG, whereas in [5] and [6] ACMs were utilized to estimate vasomotor waves and compared with blood-oxygen-level dependent imaging in MRI scanner. In [7] NIBP was combined with NIRS and ultrafast functional magnetic resonance imaging (fMRI) as an experimental tool used for glymphatic system studies. Glymphatic system is a functional waste clearance pathway, which uses the cerebrospinal fluid to remove metabolic wastes and neurotoxins from the brain along paravascular channels [45, 46]. Since the cerebrospinal fluid flux is driven by arterial pulsation, CVS abnormalities might affect brain waste clearance [7]. In the mentioned article, preliminary results on the effect of BP variations on cerebral brain dynamics are shown (Figure 28). Signals were recorded during breathing tasks. MREG (magnetic resonance encephalography) is an ultrafast fMRI sequence utilized in the study.
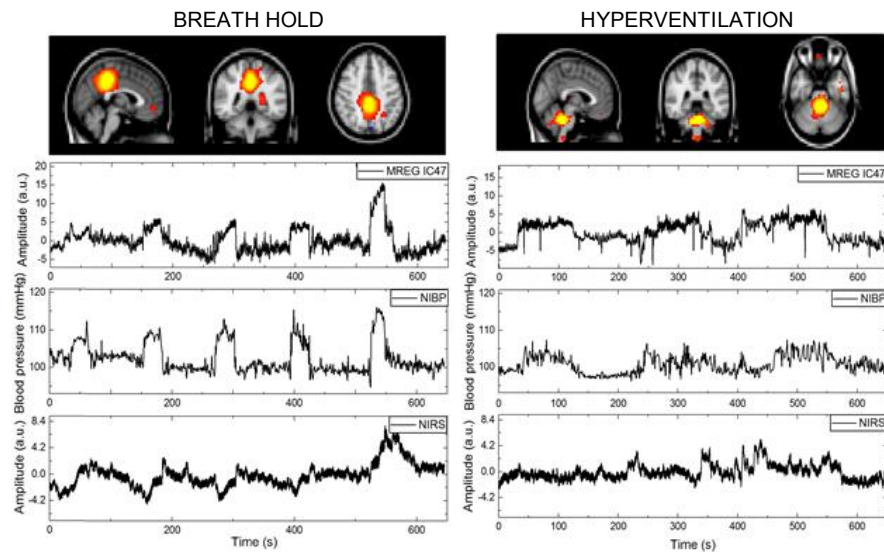

Figure 28 In the anatomical images on the top the MREG component 47 is shown. Pearson's correlation coefficient between NIBP and MREG IC47 for BH task: r=0.73, for HV task: r=0.48 [7].

Results obtained in the presented articles are very promising and suggest that the fiber optic setup might be successfully adapted as one of the modalities in further brain studies. Glymphatic system studies are planned to be continued and since it is a relatively new concept, studies in that field are of vital interest of medical doctors and researchers.

7.   CONCLUSION

PTT is an interesting factor, and its connection to various body functions is constantly being explored. Conducted research are focusing on utilizing PTT in the non-invasive BP measurement, similarly as it is done in the presented study. Due to this fact, potential usability of non-invasive fiber optics based accelerometers as a part of multimodal measurement setup appears to be fully justified.

Objective of this thesis was to compare three models of BP estimation from PTT, which was measured using fiber optics based accelerometers. Tested models were: linear regression, non-linear Moens and Korteweg model and non-linear model by Gesche et.al. Estimated BP levels were compared with IBP and Finometer readings, which were serving as a reference. The results provide preliminary information on differences between models, as well as interesting observations concerning the influence of choosing various referencing system in BP measurements. Although it was not possible to undoubtedly indicate the best method for PTT-BP modelling, thanks to this study it was possible to improve both the measurement technique and the analysis method.

Obtained results suggest, that the presented calculation methods still require further development in order to provide accurate BP values, however, can be used for observation of BP oscillations for research purposes. Compatibility with MRI and MEG environments appoints the potential of ACMs in brain research, which has been already confirmed in several publications.

8.   REFERENCES

[1]   Mutnick AH (2004) Hypertension management for the primary care clinician. , ASHP.

[2]   Payne S (2016) Cerebral autoregulation: control of blood flow in the brain. , Springer.

[3]   Myllylä T, Zacharias N, Korhonen V, Zienkiewicz A, Hinrichs H, Kiviniemi V & Walter M (2017) Multimodal brain imaging with magnetoencephalography: A method for measuring blood pressure and cardiorespiratory oscillations. Sci Rep 7(1): 172-017-00293-7. Epub 2017 Mar 14.

[4]   Myllylä T, Toronov V, Claassen J, Kiviniemi V & Tuchin V (2016) Near-Infrared Spectroscopy in Multimodal Brain Research. In: Tuchin V (ed) Handbook of Optical Biomedical Diagnostics. , SPIE Handbook vol PM 262.

[5]   Korhonen V, Hiltunen T, Myllylä T, Wang X, Kantola J, Nikkinen J, Zang Y, LeVan P & Kiviniemi V (2014) Synchronous multiscale neuroimaging environment for critically sampled physiological analysis of brain function: hepta-scan concept. Brain connectivity 4(9): 677-689.

[6]   Toronov V, Myllylä T, Kiviniemi V & Tuchin V (2013) Dynamics of the brain: Mathematical models and non-invasive experimental studies. The European Physical Journal Special Topics 222(10): 2607-2622.

[7]   Zienkiewicz A, Huotari N, Raitamaa L, Raatikainen V, Ferdinando H, Vihriälä E, Korhonen V, Myllylä T & Kiviniemi V (2017) Continuous blood pressure recordings simultaneously with functional brain imaging: studies of the glymphatic system. SPIE BiOS. , International Society for Optics and Photonics: 1006311-1006311-5.

[8]   Perdikaris P, Grinberg L & Karniadakis GE (2016) Multiscale modeling and simulation of brain blood flow. Phys Fluids 28(2): 021304.

[9]   Erkelens CD, van der Wal, Haye H, de Jong BM, Elting J, Renken R, Gerritsen M, van Laar PJ, van Deursen VM, van der Meer P & van Veldhuisen DJ (2017) Dynamics of cerebral blood flow in patients with mild non☐ischaemic heart failure. European journal of heart failure 19(2): 261-268.

[10] Myllylä TS, Elseoud AA, Sorvoja HS, Myllylä RA, Harja JM, Nikkinen J, Tervonen O & Kiviniemi V (2011) Fibre optic sensor for non☐invasive monitoring of blood pressure during MRI scanning. Journal of biophotonics 4(1☐2): 98-107.

[11] Heravi M & Khalilzadeh M (2014) Designing and Constructing an Optical System to measure Continuous and Cuffless Blood Pressure Using Two Pulse Signals. Iranian Journal of Medical Physics 11(1): 215-223.

[12] Moens AI (1878) Die Pulscurve. , Brill.

[13] Korteweg D (1878) Ueber die Fortpflanzungsgeschwindigkeit des Schalles in elastischen Röhren. Annalen der Physik 241(12): 525-542.

[14] Gesche H, Grosskurth D, Küchler G & Patzak A (2012) Continuous blood pressure measurement by using the pulse transit time: comparison to a cuff-based method. Eur J Appl Physiol 112(1): 309-315.

[15] World Health Organization (2015) Global status report on noncommunicable diseases 2014. 2014. URL: http://apps.who.int/iris/bitstream/10665/148114/1/9789241564854_eng.pdf [accessed 2016-10-11][WebCite Cache ID 6lBPfdfFf] .

[16] Parandyk W, Lewandowski D & Awrejcewicz J (2013) Human circulatory system in terms of a closed-loop hydraulic structure. , Conference book of the 12th Conference on Dynamical Systems–Theory and Applications, Lodz, Poland.

[17] Guyton J & Hall J (2011) Guyton and Hall Textbook of Medical Physiology.

[18] Pineda Pardo J (2009) Automatic Learning Procedures for Non-Invasive Blood Pressure Measurements.

[19] Islam MM, Rafi FHM, Mitul AF, Ahmad M, Rashid M & Malek, Mohd Fareq bin Abd (2012) Development of a noninvasive continuous blood pressure measurement and monitoring system. Informatics, Electronics & Vision (ICIEV), 2012 International Conference on. , IEEE: 1085-1090.

[20] Fortino G & Giampà V (2010) PPG-based methods for non invasive and continuous blood pressure measurement: An overview and development issues in body sensor networks. Medical Measurements and Applications Proceedings (MeMeA), 2010 IEEE International Workshop on. , IEEE: 10-13.

[21] Safar ME & Jankowski P (2009) Central blood pressure and hypertension: role in cardiovascular risk assessment. Clin Sci (Lond) 116(4): 273-282.

[22] Ogedegbe G & Pickering T (2010) Principles and techniques of blood pressure measurement. Cardiol Clin 28(4): 571-586.

[23] Neuman MR (2011) Measurement of blood pressure [tutorial]. Pulse, IEEE 2(2): 39-44.

[24] Solà JM (2011) Continuous non-invasive blood pressure estimation .

[25] Mukkamala R, Hahn J, Inan OT, Mestha LK, Kim C, Töreyin H & Kyal S (2015) Toward ubiquitous blood pressure monitoring via pulse transit time: theory and practice. IEEE Transactions on Biomedical Engineering 62(8): 1879-1901.

[26] Penaz J (1973) Photoelectric measurement of blood pressure, volume and flow in the finger. Digest of the 10th international conference on medical and biological engineering. , International Federation for Medical and Biological Engineering, Publishers New York 104.

[27] Sorvoja H & Myllyla R (2006) Noninvasive blood pressure measurement methods. Molecular and quantum acoustics 27: 239-264.

[28] Jagomägi K, Raamat R & Talts J (2001) Effect of altering vasoactivity on the measurement of finger blood pressure. Blood Press Monit 6(1): 33-40.

[29] McAuley D, Silke B & Farrell S (1997) Reliability of blood pressure determination with the Finapres with altered physiological states or pharmacodynamic conditions. Clinical Autonomic Research 7(4): 179-184.

[30] Payne RA (2009) Pulse transit time and the pulse wave contour as measured by photoplethysmography: the effect of drugs and exercise.

[31] Baruch MC, Warburton DE, Bredin SS, Cote A, Gerdt DW & Adkins CM (2011) Pulse Decomposition Analysis of the digital arterial pulse during hemorrhage simulation. Nonlinear biomedical physics 5(1): 1.

[32] Baruch MC, Kalantari K, Gerdt DW & Adkins CM (2014) Validation of the pulse decomposition analysis algorithm using central arterial blood pressure. Biomedical engineering online 13(1): 96.

[33] Empirical Technologies Corporation CareTaker manual. URI: https://biopac.com/wp-content/uploads/nibp-mri-caretaker-manual.pdf.

[34] Kriz J, Seba P, Martinik K & Tosnerova V (2005) Force Plate Measurement of Human Hemodynamics .

[35] Wibmer T, Doering K, Kropf-Sanchen C, Rüdiger S, Blanta I, Stoiber K, Rottbauer W & Schumann C (2014) Pulse transit time and blood pressure during cardiopulmonary exercise tests. Physiological Research 63(3): 287.

[36] Smith RP, Argod J, Pepin JL & Levy PA (1999) Pulse transit time: an appraisal of potential clinical applications. Thorax 54(5): 452-457.

[37] Sharwood-Smith G, Bruce J & Drummond G (2006) Assessment of pulse transit time to indicate cardiovascular changes during obstetric spinal anaesthesia. Br J Anaesth 96(1): 100-105.

[38] Kounalakis SN & Geladas ND (2009) The role of pulse transit time as an index of arterial stiffness during exercise. Cardiovascular Engineering 9(3): 92-97.

[39] Schmalgemeier H, Bitter T, Bartsch S, Bullert K, Fischbach T, Eckert S, Horstkotte D & Oldenburg O (2012) Pulse transit time: validation of blood pressure measurement under positive airway pressure ventilation. Sleep and Breathing 16(4): 1105-1112.

[40] Myllylä T, Korhonen V, Vihriälä E, Sorvoja H, Hiltunen T, Tervonen O & Kiviniemi V (2012) Human heart pulse wave responses measured simultaneously at several sensor placements by two MR-compatible fibre optic methods. Journal of Sensors 2012.

[41] Myllylä TS, Vihriäläa EV, Korhonenb VO & Sorvojaa HS (2013) Case study of ECG signal used as a reference signal in optical pulse transit time measurement of blood flow–The effect of different electrode placements on pulse transit time. Proc. of SPIE Vol. 8699: 869903-869901.

[42] Hughes D, Babbs CF, Geddes L & Bourland J (1979) Measurements of Young's modulus of elasticity of the canine aorta with ultrasound. Ultrason Imaging 1(4): 356-367.

[43] Lass J, Meigas I, Karai D, Kattai R, Kaik J & Rossmann M (2004) Continuous blood pressure monitoring during exercise using pulse wave transit time measurement. Engineering in Medicine and Biology Society, 2004. IEMBS'04. 26th Annual International Conference of the IEEE. , IEEE 1: 2239-2242.

[44] Masè M, Mattei W, Cucino R, Faes L & Nollo G (2011) Feasibility of cuff-free measurement of systolic and diastolic arterial blood pressure. J Electrocardiol 44(2): 201-207.

[45] Iliff JJ, Wang M, Liao Y, Plogg BA, Peng W, Gundersen GA, Benveniste H, Vates GE, Deane R, Goldman SA, Nagelhus EA & Nedergaard M (2012) A paravascular pathway facilitates CSF flow through the brain parenchyma and the clearance of interstitial solutes, including amyloid beta. Sci Transl Med 4(147): 147ra111.

[46] Venkat P, Chopp M & Chen J (2016) New insights into coupling and uncoupling of cerebral blood flow and metabolism in the brain. Croat Med J 57(3): 223-228.